Reaction Mechanism in the Stereospecific 1,4-Polymerization of Butadiene with Ziegler−Natta Type Catalysts of Early Transition Metals: Comprehensive Density Functional Investigation for the Cationic [Ti^{III}Cp(polybutadienyl)(butadiene)]$^+$ Active Catalyst

Sven Tobisch†

Institut für Anorganische Chemie der Martin-Luther-Universität Halle-Wittenberg, Fachbereich Chemie, Kurt-Mothes-Strasse 2, D-06120 Halle, Germany

Received January 24, 2003

A comprehensive theoretical investigation of the entire catalytic reaction course of the 1,4-polymerization of 1,3-butadiene assisted by the cationic [Ti^{III}Cp(polybutadienyl)(butadiene)]$^+$ active catalyst complex, employing a gradient-corrected DFT method, is presented. Critical elementary processes for a tentative catalytic cycle have been scrutinized, taking into account monomer insertion, allylic anti-syn isomerization, and the monomer uptake. The present investigation examines, in terms of the located key structures and the energy profile of individual elementary steps, the role played by η^3-π-butenyl− and η^1-σ-butenyl−Ti^{III} species as possible intermediates in the catalytic reaction course. The mechanistic insights are improved by clarifying the following aspects. (1) The chain propagation preferably proceeds via *cis*-butadiene insertion into the η^3-butenyl−Ti^{III} bond, thus verifying the π-allyl-insertion mechanism as being operative. (2) The alternative insertion commencing from the s-trans configuration of butadiene is seen to be kinetically disfavored, with thermodynamic considerations found to be less decisive. (3) The allylic anti-syn isomerization is indicated to be much slower than the monomer insertion step. (4) The regeneration of the active catalyst species proceeds via a facile monomer uptake in the *anti*-η^3-butenyl−Ti^{III} insertion product, which occurs with preservation of the η^3-π coordination mode of the terminal group of the growing polybutadienyl chain. (5) The formation of *anti*-η^3-butenyl species as the result of the favorable *cis*-butadiene insertion and the slow allylic isomerization are the critical factors for the nearly exclusive generation of *cis*-1,4-polybutadiene, notwithstanding the comparable reactivity of *anti*-η^3- and *syn*-η^3-butenyl forms. (6) The formation of an isotactic *cis*-1,4-polymer is rationalized in terms of the higher reactivity of the *cis*-1,3-diene in its prone orientation together with the regulating influence of the axial Cp ligand.

Introduction

The catalytic polymerization of 1,3-dienes assisted by transition-metal compounds is a key process in the worldwide chemistry industry.[1] Both structurally defined allyl−transition-metal complexes, as well as Ziegler−Natta catalyst systems, have been established that actively catalyze the stereoselective polymerization of 1,3-dienes.[2] These catalysts are superior to other initiators in the 1,3-diene polymerization, due to their ability to catalyze the C−C bond formation in a highly chemo-, regio-, and stereoselective fashion.[3]

Titanium-based Ziegler−Natta systems, with aluminum alkyls or aluminoxanes as cocatalysts, have been demonstrated to be versatile and efficient catalysts for the polymerization of 1,3-dienes.[2e,4] The catalyst system $CpTiCl_3$/MAO, in particular, is one of the most carefully studied Ziegler−Natta catalysts, has been experimentally examined in great detail, and has been found to assist both the homo- and copolymerization of a wide range of different 1,3-dienes[5,6] as well as the generation of polystyrene[7] and of styrene−butadiene copolymers.[8]

† E-mail: tobisch@chemie.uni-halle.de.

(1) La Flair, R. T.; Wolf, U. U. In *Ullmann's Encyclopedia of Industrial Chemistry*, 5th ed.; Verlag Chemie: Weinheim, Germany, 1993; Vol. A23, pp 273−282.

(2) (a) Porri, L.; Natta, G.; Gallazzi, M. C. *Chim. Ind.* **1964**, *46*, 428. (b) Dolgoplosk, B. A.; Babitskii, B. D.; Kormer, V. A.; Lobach, M. I.; Tinyakova, E. T. *Dokl. Akad. Nauk SSSR* **1965**, *164*, 1300. (c) Wilke, G.; Bogdanovic, B.; Hardt, P.; Heimbach, P.; Keim, W.; Kröner, M.; Oberkirch, W.; Tanaka, K.; Steinrucke, E.; Walter, D.; Zimmermann, H. *Angew. Chem., Int. Ed. Engl.* **1966**, *5*, 151. (d) Durand, J. P.; Dawans, F.; Teyssie, Ph. *J. Polym. Sci. B* **1968**, *6*, 757. (e) Porri, L.; Giarrusso, A. In *Comprehensive Polymer Science*; Eastmond, G. C., Ledwith, A., Russo, S., Sigwalt, B., Eds.; Pergamon: Oxford, U.K., 1989; Vol. 4, Part II, pp 53−108. (f) Taube, R.; Windisch, H.; Maiwald, St. *Macromol. Symp.* **1995**, *89*, 395−409.

(3) (a) Teyssie, Ph.; Julemont, M.; Thomassin, J. M.; Walkiers, E.; Warin, R. In *Coordination Polymerization*; Chien, J. C. W., Ed.; Academic Press: New York, 1975; pp 327−347. (b) Boor, J., Jr. *Ziegler−Natta Catalysts and Polymerizations*; Academic Press: New York, 1979. (c) Porri, L. In *Structural Order in Polymers*; Ciardelli, F., Giusti, P., Eds.; Pergamon Press: Oxford, U.K., 1981; pp 51−62.

(4) (a) Teyssie, Ph.; Dawans, F. In *The Stereo Rubbers*; Saltman, W. M., Ed.; Wiley: New York, 1977; pp 79−138. (b) Dolgoplosk, B. A. *Sov. Sci. Rev., Sect. B* **1980**, *2*, 203−282.

10.1021/om030059p CCC: $25.00
Publication on Web 05/17/2003

There is considerable experimental evidence, although not firmly established, that the cationic $[Ti^{III}Cp(polydienyl)(monomer)]^+$ complex acts as the catalytically active species in 1,3-diene homo- and copolymerization.[5b,7e] Under typical reaction conditions (~20 °C, Ti:MAO ≈ 1:1000) this catalyst promotes the generation of *cis*-1,4-polybutadiene as the main product (~80%) together with a minor portion of 1,2-polymer units.[5a,b,6] Furthermore, the polymer product of the terminally substituted (*Z*)-1,3-pentadiene consists almost entirely of cis-1,4-units of predominantly isotactic structure.[5a−c,6]

Despite the paramount importance of Ziegler−Natta type catalysts of early transition metals in the manufacturing process of polydienes and the considerable amount of experimental studies for these systems, relatively little is known about the mechanistic aspects of the polymerization process, in particular for the mechanism of stereoregulation. Only a few mechanistic details have been firmly established for these catalysts. Furthermore, theoretical mechanistic investigations on 1,3-diene polymerization are scarce, when compared to the abundance of theoretical studies on olefin polymerization. Computational studies were previously conducted on 1,3-diene polymerization mediated by the $CpTiCl_3$/MAO catalyst system, where the focus was on the *cis*-butadiene insertion and on the generation of the active catalyst species.[9]

The present study explores theoretically critical elementary processes of the entire catalytic reaction course for 1,4-polymerization of 1,3-butadiene assisted by the $[Ti^{III}Cp(polybutadienyl)(butadiene)]^+$ catalyst complex. The following key elementary steps of the polymerization cycle are explicitly scrutinized: (1) monomer insertion into the butenyl−Ti^{III} bond along the competing pathways for generation of trans-1,4- and cis-1,4-polymer units, (2) interconversion of isomeric anti and syn forms of the butenyl−Ti^{III} bond, and (3) monomer uptake occurring in the insertion product affording the catalytically active species, the butadiene π-complex. The role played by these elementary processes in the mechanism of the cis−trans stereoregulation is elucidated. Furthermore, for the key species that are involved in the several elementary processes, the thermodynamic stability and kinetic reactivity of isomers have been explicitly explored, originating from different modes of monomer coordination (i.e. monodentate or bidentate mode of *s-cis*- and *s-trans*-butadiene), and the anti and syn configurations of the butenyl−Ti^{III} bond have been explicitly explored. The present study is aimed at clarifying the following intriguing mechanistic questions that are still unresolved after both experimental and previous theoretical investigations.

(1) Which of the two proposed mechanisms for the insertion of butadiene into the transition-metal−butenyl bond, i.e. the σ-allyl- or the π-allyl-insertion mechanism (vide infra), is operative for the catalyst under investigation?

(2) Which of the important steps of the catalytic reaction course, namely the monomer insertion step, the allylic anti−syn isomerization, or the formation of the active catalyst species by monomer uptake, must be regarded as being rate-controlling?

(3) Which factors are decisive for the cis−trans stereoregulation of the 1,4-polymerization of 1,3-butadiene, and what role do the individual elementary steps play in this regard?

(4) What factors determine the tacticity of the polydiene products of terminally monosubstituted butadienes?

(5) Which of the several species that are involved in the polymerization cycle represent the resting state of the catalyst under catalytic reaction conditions?

Addressing these questions will contribute to a more detailed understanding of the cis−trans regulation, in terms of thermodynamic and kinetic aspects, of the butadiene 1,4-polymerization assisted by the prototype cationic allyltitanium(III) catalyst $[Ti^{III}(C_5H_5)(RC_3H_4)(C_4H_6)]^+$. Furthermore, this study is aimed at enhancing the understanding of the catalytic structure−reactivity relationships in the transition-metal-assisted stereoselective polymerization of 1,3-dienes. In our previous theoretical explorations of the entire catalytic cycle for all important types of experimentally verified allylnickel(II) catalysts,[10,11] we were able to deduce a comprehensive insight into the relationships between the catalyst's structure and its reactivity as well its stereoselectivity in the 1,4-polymerization of 1,3-dienes, for this important class of active late-transition-metal catalysts. These insights are intended to be extended by the present elucidation of the catalytic structure−reactivity relationships for an experimentally well-characterized early-transition-metal-based catalyst. The focus of the present study is entirely on 1,4-polymerization, while the catalytic cycle for 1,2-polymerization of 1,3-dienes will be the subject of a forthcoming investigation.

(5) (a) Oliva, L.; Longo, P.; Grassi, A.; Ammendola, P.; Pellecchia, C. *Makromol. Chem., Rapid Commun.* **1990**, *11*, 519. (b) Ricci, G.; Italia, S.; Giarusso, A.; Porri, L. *J. Organomet. Chem.* **1993**, *451*, 67. (c) Ricci, G.; Italia, S.; Porri, L. *Macromolecules* **1994**, *27*, 868. (d) Meille, S. V.; Capelli, S.; Ricci, G. *Macromol. Rapid Commun.* **1995**, *16*, 891. (e) Longo, P.; Oliva, P.; Proto, A.; Zambelli, A. *Gazz. Chim. Ital.* **1996**, *377*, 126. (f) Longo, P.; Proto, A.; Oliva, P.; Zambelli, A. *Macromolecules* **1996**, *29*, 5500. (g) Longo, P.; Grisi, F.; Proto, A.; Zambelli, A. *Macromol. Rapid Commun.* **1997**, *18*, 183. (h) Ricci, G.; Porri, L. *Macromol. Chem. Phys.* **1997**, *198*, 3647. (i) Longo, P.; Guerra, G.; Grisi, F.; Pizzuti, S.; Zambelli, A. *Macromol. Chem. Phys.* **1998**, *199*, 149.

(6) (a) Porri, L.; Giarrusso, A.; Ricci, G. *Makromol. Chem., Macromol. Symp.* **1993**, *66*, 231. (b) Porri, L.; Giarrusso, A. *Macromol. Symp.* **1995**, *89*, 383. (c) Porri, L.; Ricci, G.; Giarrusso, A. In *Metalorganic Catalysts for Synthesis and Polymerization*; Kaminsky, W., Ed.; Springer-Verlag: Berlin, Heidelberg, 1999; pp 519−530.

(7) (a) Ishikara, N.; Seimya, T.; Kuramoto, M.; Uoi, M. *Macromolecules* **1986**, *19*, 2465. (b) Pellecchia, C.; Longo, P.; Grassi, A.; Ammendola, P.; Zambelli, A. *Makromol. Chem., Rapid Commun.* **1987**, *8*, 277. (c) Ishikara, N.; Kuramoto, M.; Uoi, M. *Macromolecules* **1988**, *21*, 3356. (d) Zambelli, A.; Oliva, L.; Pellecchia, C. *Macromolecules* **1989**, *22*, 2129. (e) Zambelli, A.; Pellecchia, C.; Oliva, L.; Longo, P.; Grassi, A. *Makromol. Chem.* **1991**, *192*, 223. (f) Chien, J. C. M.; Salajka, Z.; Dong, S. *Macromolecules* **1992**, *25*, 3199.

(8) (a) Pellecchia, C.; Proto, A.; Zambelli, A. *Macromolecules* **1992**, *25*, 4450. (b) Zambelli, A.; Proto, A.; Longo, P.; Oliva, P. *Macromol. Chem. Phys.* **1994**, *195*, 2623. (b) Zambelli, A.; Caprio, M.; Grassi, A.; Bowen, D. E. *Macromol. Chem. Phys.* **2000**, *201*, 393.

(9) (a) Guerra, G.; Cavallo, L.; Corradini, P.; Fusco, R. *Macromolecules* **1997**, *30*, 677. (b) Peluso, A.; Improta, R.; Zambelli, A. *Macromolecules* **1997**, *30*, 2219. (c) Improta, R.; Garzillo, C.; Peluso, A. *THEOCHEM* **1998**, *426*, 249. (d) Improta, R.; Peluso, A. *Macromolecules* **1999**, *32*, 6852. (e) Peluso, A.; Improta, R.; Zambelli, A. *Organometallics* **2000**, *19*, 411. (f) Costabile, C.; Milano, G.; Cavallo, L.; Guerra, G. *Macromolecules* **2001**, *34*, 7952.

(10) (a) Tobisch, S.; Bögel, H.; Taube, R. *Organometallics* **1996**, *15*, 3563. (b) Tobisch, S.; Bögel, H.; Taube, R. *Organometallics* **1998**, *17*, 1177. (c) Tobisch, S.; Taube, R. *Organometallics* **1999**, *18*, 5204. (d) Tobisch, S.; Taube, R. *Chem. Eur. J.* **2001**, *7*, 3681. (e) Tobisch, S. *Chem. Eur. J.* **2002**, *8*, 4756.

(11) Tobisch, S. *Acc. Chem. Res.* **2002**, *35*, 96.

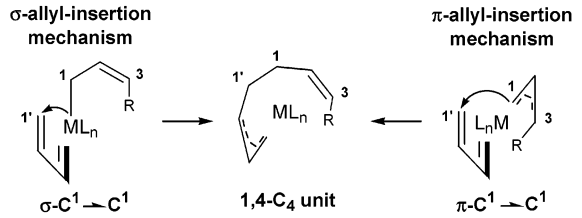

Figure 1. Transition-metal-assisted C−C bond formation between butadiene and the butenyl group achieved as a C^1-C^1 linkage according to the σ-allyl and the π-allyl insertion mechanism (R denotes the growing polybutadienyl chain).

General Catalytic Reaction Cycle

First, the peculiar mechanistic aspects of 1,3-diene polymerization, those important for the understanding of the catalytic process, will be briefly outlined.[11−13] Transition-metal-catalyzed 1,3-diene polymerization is an insertion polymerization.[14] As established convincingly for the allylnickel(II)-catalyzed 1,3-diene polymerization,[15] the chain growth proceeds in consecutive steps, starting with the coordination of the monomer and followed by intramolecular migratory insertion into the butenyl−transition-metal bond. The η^3-π and η^1-σ coordination modes, in general, can represent the reactive form of the butenyl−transition-metal bond, as illustrated in Figure 1. Cossee and Arlman suggested that the butenyl group reacts from the η^1-σ mode,[16] while the C−C bond formation should be occurring via monomer insertion into the η^3-π-butenyl−transition-metal bond according to Taube.[12,17] Until recently, the σ-allyl-insertion mechanism[16] was generally believed to be the preferred mechanistic alternative for the monomer insertion step in the 1,3-diene polymerization.[3,9a−e,18] The π-allyl-insertion mechanism, however, was firmly established in our recent theoretical studies as being the operative one of the two mechanistic suggestions in the case of the allylnickel(II)-catalyzed polymerization of 1,3-dienes.[10,11]

Butadiene can coordinate in two modes: monodentate (η^2) or bidentate (η^4), from either the s-trans or the s-cis configuration. The η^4-cis and η^4-trans coordination of 1,3-butadiene in group 4 complexes has been established by several X-ray structural characterizations.[19] According to the generally accepted anti-cis and syn-trans correlation,[2e] the configuration of the terminal η^3-butenyl group in the kinetic insertion product is determined by the configuration of the inserting monomer. An *anti*- or *syn*-η^3-butenyl terminal group is formed by butadiene insertion proceeding from the s-cis (anti insertion) or s-trans (syn insertion) configuration, respectively. Additionally, butadiene insertion gives rise to a cis or a trans double bond in the newly formed polymer unit of the growing polymer chain, when commencing from an *anti*- or *syn*-butenyl group. Both aspects of the anti-cis and syn-trans correlation are schematically depicted in Figure 2.

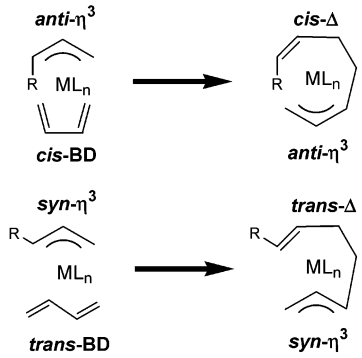

Figure 2. Anti-cis and syn-trans correlation of the transition-metal-assisted 1,4-polymerization of 1,3-butadiene (R denotes the growing polybutadienyl chain).

The proclivity of the two isomeric anti and syn forms of the butenyl−transition-metal bond to undergo monomer insertion in relation to their mutual interconversion via allylic isomerization has a crucial impact on the cis−trans regulation for the 1,4-polymerization of 1,3-dienes.

On the basis of these mechanistic aspects, a general catalytic reaction scheme of the 1,4-polymerization of 1,3-butadiene with the cationic $[Ti^{III}(C_5H_5)(RC_3H_4)(C_4H_6)]^+$ complex as the active catalyst is outlined in Scheme 1. The active catalyst complex **2** is formed from the $CpTiCl_3$/MAO Ziegler−Natta precatalysts **1** under the influence of excess methylaluminoxanes and of butadiene during the initiation phase of the polymerization process. With the catalytically active butadiene π-complex **2** as starting material, the monomer insertion process can occur along two routes for *cis*-butadiene and *trans*-butadiene insertion. For each of the two routes, there are two competing paths for butadiene insertion into either the *anti*- or *syn*-butenyl−Ti^{III} bond via the transition states **3a** and **3s**, giving rise to cis-1,4 (k_c) and trans-1,4 (k_t) polymer units. Along the *cis*-butadiene insertion route (via the k_c(cis) and k_t(cis) paths), an *anti*-butenyl group is regenerated as the reactive terminal

(12) Taube, R.; Sylvester, G. In *Applied Homogeneous Catalysis with Organometallic Complexes*; Cornils, B., Herrmann, W. A., Eds.; VCH: Weinheim, Germany, 1996; pp 280−317.
(13) Porri, L.; Giarrusso, A.; Ricci, G. *Prog. Polym. Sci.* **1991**, *16*, 405.
(14) Pino, P.; Giannini, U.; Porri, L. In *Encyclopedia of Polymer Science and Engineering*, 2nd ed.; Wiley: New York, 1987; Vol. 8, pp 147−220.
(15) (a) Lobach, M. I.; Kormer, V. A.; Tsereteli, I. Yu.; Kondoratenkov, G. P.; Babitskii, B. D.; Klepikova, V. I. *J. Polym. Sci., Polym. Lett.* **1971**, *9*, 71. (b) Warin, R.; Teyssié, Ph.; Bourdauduraq, P.; Dawans, F. *J. Polym. Sci., Polym. Lett.* **1973**, *11*, 177.
(16) (a) Cossee, P. In *Stereochemistry of Macromolecules*; Ketley, A. D., Ed.; Marcel Dekker: New York, 1967; Vol. 1, pp 145−175. (b) Arlman, E. J. *J. Catal.* **1966**, *5*, 178−189.
(17) (a) Taube, R.; Gehrke, J.-P.; Böhme, P. *Wiss. Zeitschr. Techn. Hochschule Leuna-Merseburg* **1987**, *39*, 310. (b) Taube, R.; Schmidt, U.; Gehrke, J.-P.; Böhme, P.; Langlotz, J.; Wache, St. *Makromol. Chem. Makromol. Symp.* **1993**, *66*, 245−260. (c) Taube, R. In *Metalorganic Catalysts for Synthesis and Polymerization*; Kaminsky, W., Ed.; Springer-Verlag: Berlin, Heidelberg, 1999; p 531.
(18) Porri, L.; Giarrusso, A.; Ricci, G. *J. Polym. Sci., Part A* **1994**, *36*, 1421.
(19) (a) Wreford, S. S.; Whitney, J. F. *Inorg. Chem.* **1981**, *20*, 3918. (b) Erker, G.; Engel, K.; Krüger, C.; Chiang, A. *Chem. Ber.* **1982**, *115*, 3311. (c) Erker, G.; Berg, K.; Krüger, C.; Müller, G.; Angermund, K.; Benn, R.; Schroth, G. *Angew. Chem., Int. Ed. Engl.* **1984**, *23*, 455. (d) Yamamoto, H.; Yasuda, H.; Tatsami, K.; Lee, K.; Nakamura, A.; Chen, J.; Kai, Y.; Kasai, N. *Organometallics* **1989**, *8*, 105. (e) Fryzuk, M. D.; Haddad, T. S.; Rettig, S. J. *Organometallics* **1989**, *8*, 1723. (f) Wielstra, Y.; Gambarotta, S. *Organometallics* **1990**, *9*, 572. (g) Erker, G. *J. Organomet. Chem.* **1990**, *400*, 185. (h) Spencer, M. D.; Wilson, S. R.; Girolami, G. S. *Organometallics* **1997**, *16*, 3055. (i) Erker, G.; Wichler, J.; Engl, K.; Rosenfeldt, F.; Dietrich, W.; Krüger, C. *J. Am. Chem. Soc.* **1980**, *102*, 6344. (j) Yasuda, H.; Kajihara, Y.; Mashima, K.; Nagasuna, K.; Lee, K.; Nakamura, A. *Organometallics* **1982**, *1*, 338. (k) Erker, G.; Wicher, J.; Engel, K.; Krüger, C. *Chem. Ber.* **1982**, *115*, 3300. (l) Dorf, U.; Erker, G. *Organometallics* **1983**, *2*, 462. (m) Czisch, P.; Erker, G.; Korth, H.; Sustmann, R. *Organometallics* **1984**, *3*, 945. (n) Dahlmann, M.; Erker, G.; Fröhlich, R.; Meyer, O. *Organometallics* **1999**, *18*, 4459.

Scheme 1. General Catalytic Reaction Cycle of the 1,4-Polymerization of 1,3-Butadiene with the Cationic $[Ti^{III}(C_5H_5)(RC_3H_4)(C_4H_6)]^+$ Complex as the Active Catalyst[a]

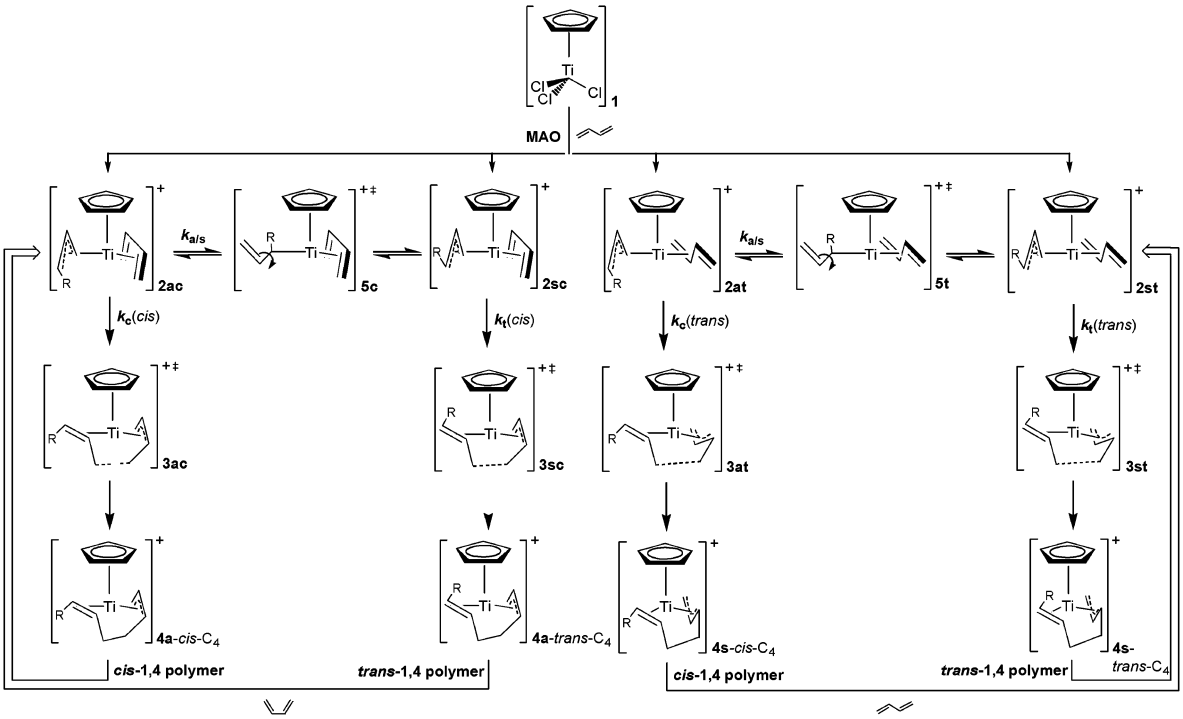

[a] Competitive paths for *cis*- and *trans*-butadiene insertion into the *anti*-butenyl−Ti^{III} bond (along k_c(cis) and k_c(trans)) affording cis-1,4-polymer units and into the *syn*-butenyl−Ti^{III} bond (along k_t(cis) and k_t(trans)) affording trans-1,4-polymer units together with the allylic anti−syn isomerization (along $k_{a/s}$) are included. The conformations of the key species (for notation see the text) involved along different reaction paths are schematically depicted.

end of the growing polybutadienyl chain in the insertion products **4a**, from which the chain-growth cycle repeats with formation of **2ac** from **4a** by *cis*-butadiene uptake. The insertion product **4s** with a *syn*-butenyl-terminated polybutadienyl chain is generated in the reaction route that involves the insertion of *trans*-butadiene (with the competing k_c(trans) and k_t(trans) paths), giving rise to **2st** via subsequent uptake of *trans*-butadiene as the starting point for a new polymerization cycle within this route. The isomeric *anti*- and *syn*-butenyl forms of the different species in each of the two routes are in equilibrium and can be interconverted via allylic isomerization. This is shown in Scheme 1 to occur in the butadiene π-complex via the transition states **5c** and **5t**, respectively. It becomes evident from Scheme 1 that allylic isomerization is an indispensable process for the generation of *trans*-1,4-polymer units (via k_t(cis)) along the reaction route for *cis*-butadiene insertion, as well as for the production of a *cis*-1,4-polybutadiene (via k_c(trans)) in the case where the alternative insertion of *trans*-butadiene is more feasible.

Computational Model and Method

Model. We modeled the real cis-1,4-regulating cationic $[Ti^{III}(C_5H_5)(RC_3H_4)(C_4H_6)]^+$ active catalysts by the cationic $[Ti^{III}(C_5H_5)(C_4H_7)(C_4H_6)]^+$ complex, where R = CH_3 was chosen as a suitable and computationally practicable model for the growing polybutadienyl chain. Preliminary investigations indicate that the polybutadienyl chain has no tendency to coordinate via its double bonds to the Ti^{III} center in the butadiene π-complexes. Thus, our catalyst model should allow an adequate description of the stability and the reactivity of the isomeric anti and syn forms of the reactive terminal group of the polybutadienyl chain.

The investigations have focused on important elementary processes of the polymerization cycle: the monomer insertion step, the allylic isomerization process, and the monomer uptake process **4** → **2**. The initialization step, that is, the formation of the active catalyst complex **2** from the Ziegler−Natta type precatalyst **1**, will, however, not be considered. The effect of the solvent and the counterion was neglected in the present study, which is aimed at the elucidation of the principal mechanistic aspects of the polymerization process.

The intrinsic energy for inserting *cis*-butadiene into a C−C bond (the energy gain that results from breaking one C−C double bond and forming a C−C single bond during the insertion) without a catalytically active transition-metal center was estimated as the average value of the exothermicities which were obtained for the general reaction according to

$$C_4H_7-(C_4H_6)_n-C_4H_7 + C_4H_6 \rightarrow C_4H_7-(C_4H_6)_{n+1}-C_4H_7\ (n = 0-2) \quad (1)$$

This amounts to 20.3 kcal mol^{-1} (ΔE) and 17.4 kcal mol^{-1} (ΔH), in good agreement with the experimental value of 18.7 kcal mol^{-1} (ΔH) for the heat of 1,4-polymerization.[20]

Method. The entire catalytic cycle for polymerization is theoretically explored by employing a gradient-corrected density functional (DFT) method. The unrestricted open-shell formalism was applied in all reported calculations, which were performed by using the TURBOMOLE program package developed by Häser and Ahlrichs.[21] The local exchange-correlation potential by Slater[22a,b] and Vosko et al.[22c] was augmented with gradient-corrected functionals for electron exchange according to Becke[22d] and correlation according to

(20) Robert, D. E. *J. Res. Natl. Bur. Stand.* **1950**, *44*, 221.

(21) (a) Ahlrichs, R.; Bär, M.; Häser, M.; Horn, H.; Kölmel, C. *Chem. Phys. Lett.* **1989**, *162*, 165. (b) Treutler, O.; Ahlrichs, R. *J. Chem. Phys.* **1995**, *102*, 346. (c) Eichkorn, K.; Treutler, O.; Öhm, H.; Häser, M.; Ahlrichs, R. *Chem. Phys. Lett.* **1995**, *242*, 652.

Perdew[22e] in a self-consistent fashion. This gradient-corrected density functional is usually termed BP86 in the literature. In recent benchmark computational studies it was shown that the BP86 functional gives results in excellent agreement with the best wave function based method available today, for the class of reactions investigated here.[23]

For all atoms a standard all-electron basis set of triple-ζ quality for the valence electrons augmented with polarization functions was employed for the geometry optimization and the saddle-point search. The Wachters 14s/9p/5d set[24a] supplemented by two diffuse p[24a] and one diffuse d function[24b] contracted to (62111111/5111111/3111) was used for titanium, and standard TZVP basis sets[24c] were used for carbon (a 10s/6p/1d set contracted to (7111/411/1)) and for hydrogen (a 5s/1p set contracted to (311/1)). The frequency calculations were done by using standard DZVP basis sets,[24c] which consist of a 15s/9p/5d set contracted to (63321/531/41) for titanium, a 9s/5p/1d set contracted to (621/41/1) for carbon, and a 5s set contracted to (41) for hydrogen, for DZVP-optimized structures. The corresponding auxiliary basis sets were used for fitting the charge density.[24c,d] This is the standard computational methodology utilized throughout this paper.

Stationary Points. The geometry optimization and the saddle-point search were carried out at the BP86 level of approximation by utilizing analytical/numerical gradients/Hessians according to standard algorithms. No symmetry constraints were imposed in any case. The stationary points were identified exactly by the curvature of the potential-energy surface at these points corresponding to the eigenvalues of the Hessian. The reaction and activation enthalpies and free energies (ΔH, $\Delta H^{\ddagger}$ and ΔG, $\Delta G^{\ddagger}$ at 298 K and 1 atm) were calculated for the most stable isomers of each of the key species of the entire catalytic reaction. The educt and product that correspond directly to the located transition-state structure were verified by following the reaction pathway going downhill to both sides from slightly relaxed transition-state structures.

Labeling of the Molecules. Important species of the catalytic cycle were labeled with the arabic numbers given in Scheme 1: viz. the precatalyst **1**, the catalytically active butadiene π-complex **2**, the transition state for monomer insertion **3**, the insertion product **4**, and the transition state for allylic isomerization **5**. The *anti*- and *syn*-butenyl forms for **2**−**4** are labeled by **a** and **s**, respectively. An additional **c** and **t** is used for **2**−**5** in order to distinguish between the species that are involved in reaction routes for insertion of *cis*- and *trans*-butadiene, respectively. The configurations of the two reacting moieties, which are butadiene (s-cis and s-trans) and the butenyl group (anti and syn form), as well as their enantioface involved in the chain propagation cycle, are of importance for the stereocontrol of the polymerization process. The enantiomeric forms of the butenyl−Ti^{III} and the butadiene−Ti^{III} coordination are schematically depicted in Figure 3. In addition to the commonly used *Re*/*Si* terminology[25] these enantiomers can also be denoted as supine (exo) and prone (endo).[26,27] Furthermore, different mutual arrangements of the two reacting moieties have to be taken into account. The formation of the C−C bond between the butenyl group and *cis*-butadiene, for example, can occur from the two moieties in supine (SS) or prone (PP) orientation or between different orientations of either SP or PS mutual arrangement. The several isomers that are possible for each species were carefully explored.

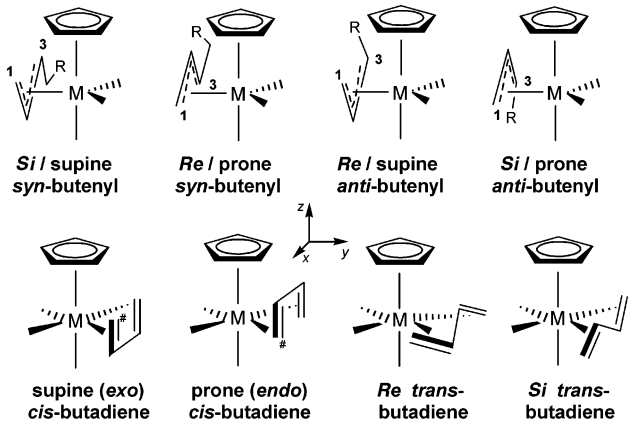

Figure 3. Two enantiomeric forms of the η^3-butenyl−transition-metal (anti and syn configurations) and the η^4-butadiene−transition-metal (s-cis and s-trans configurations) coordination.[27]

Table 1. Calculated Gibbs Free Energy Profile (ΔG, $\Delta G^{\ddagger}$ in kcal mol^{-1}) for the Monomer Insertion Step of the 1,4-Polymerization of 1,3-Butadiene for the $[Ti^{III}(\eta^5\text{-}C_5H_5)(\eta^3\text{-}C_4H_7)(\eta^4\text{-}C_4H_6)]^+$ Active Catalyst Complex[a,b]

isomer	2	3	4
Route for *cis*-Butadiene Insertion			
anti-SS	5.2	27.4	−6.1
anti-PS	6.1	22.6	−3.1
anti-SP	5.9	12.1	−3.1
anti-PP	4.4	7.4	−6.1
syn-SS	0.5	20.9	−5.9
syn-PS	1.6	18.2	−4.4
syn-SP	1.6	6.1	−4.4
syn-PP	0.0	6.0	−5.9
Route for *trans*-Butadiene Insertion			
anti-*Re*/*Re*	6.6	27.9	−1.9
anti-*Si*/*Re*	6.0	22.4	−4.9
anti-*Re*/*Si*	6.5	17.8	−2.3
anti-*Si*/*Si*	5.6	14.6	−3.4
syn-*Si*/*Re*	4.3	22.1	−4.5
syn-*Re*/*Re*	0.9	18.6	−3.4
syn-*Si*/*Si*	3.5	11.9	−1.1
syn-*Re*/*Si*	0.6	16.4	−1.1

[a] The several isomers are denoted according to the enantiofaces of the two reacting moieties that are involved in the insertion process in the following way: anti and syn refers to the configuration of the butenyl group followed by a description of the enantioface first of the butenyl group and second of butadiene either in the supine (S), prone (P) or in the *Re*/*Si* terminology. [b] Free energies relative to the $[Ti^{III}(\eta^5\text{-}C_5H_5)(syn\text{-}\eta^3\text{-}C_4H_7)(\eta^4\text{-}cis\text{-}C_4H_6)]^+$ PP isomer of **2**.

Results and Discussion

We shall start our investigation by exploring important elementary processes of the catalytic reaction course, namely the monomer insertion, allylic isomerization, and monomer uptake, first with a detailed examination of the insertion routes for *cis*- and *trans*-butadiene occurring along competitive paths. The free-energy profile for this process is collected in Table 1, and the key species that are involved along the most

(22) (a) Dirac, P. A. M. *Proc. Cambridge Philos. Soc.* **1930**, *26*, 376. (b) Slater, J. C. *Phys. Rev.* **1951**, *81*, 385. (c) Vosko, S. H.; Wilk, L.; Nussair, M. *Can. J. Phys.* **1980**, *58*, 1200. (d) Becke, A. D. *Phys. Rev.* **1988**, *A38*, 3098. (e) Perdew, J. P. *Phys. Rev. B* **1986**, *B33*, 8822; *Phys. Rev. B* **1986**, *34*, 7406.

(23) Jensen, V. R.; Børve, K. *J. Comput. Chem.* **1998**, *19*, 947.

(24) (a) Wachters, A. H. J. *J. Chem. Phys.* **1970**, *52*, 1033. (b) Hay, P. J. *J. Chem. Phys.* **1977**, *66*, 4377. (c) Godbout, N.; Salahub, D. R.; Andzelm, J.; Wimmer, E. *Can. J. Chem.* **1992**, *70*, 560. (d) TURBOMOLE basis set library.

(25) Hanson, K. R. *J. Am. Chem. Soc.* **1966**, *88*, 2731.

(26) Yasuda, H.; Nakamura, A. *Angew. Chem., Int. Ed. Engl.* **1987**, *16*, 723.

(27) For the η^3-π-butenyl−transition-metal coordination the supine/prone notation[26] is given in addition to the *Re*/*Si* terminology.[25] The *Re*/*Si* terminology is applied with regard to the chirality of the butenyl group's C^3 atom.

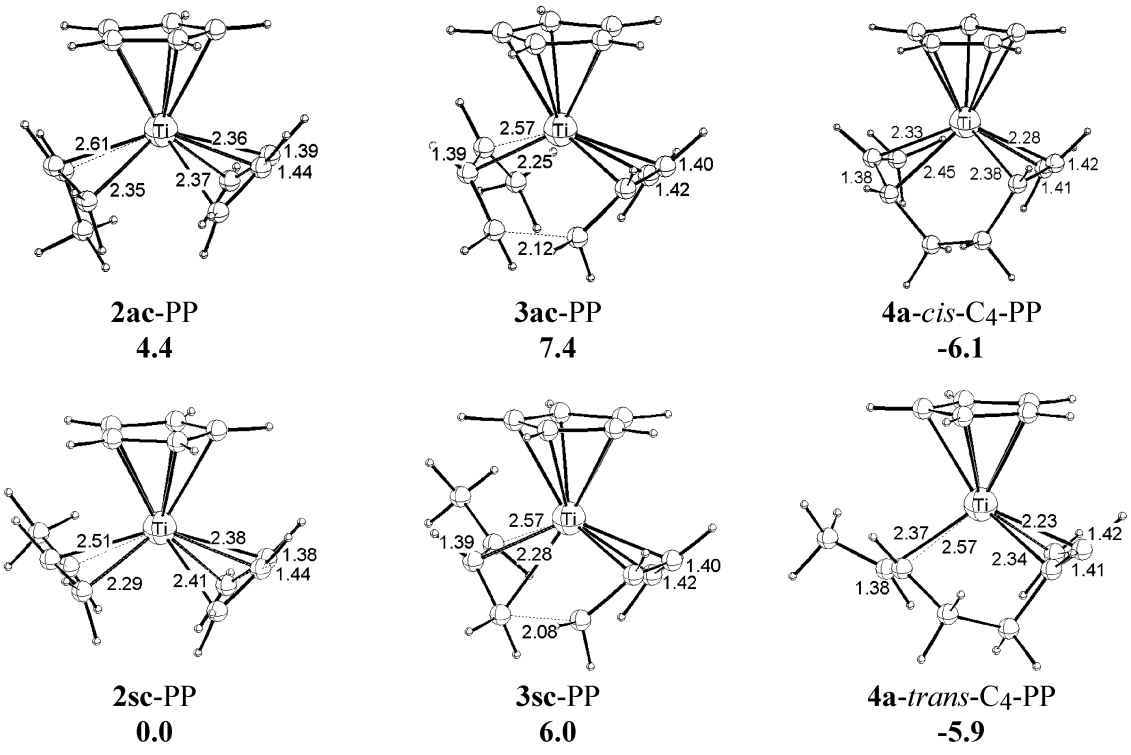

Figure 4. Selected geometric parameters (Å) of the optimized structures of key species for *cis*-butadiene insertion into the η^3-*anti*-butenyl−Ti^{III} bond (top) and into the η^3-*syn*-butenyl−Ti^{III} bond (bottom) of the $[Ti^{III}(\eta^5\text{-}C_5H_5)(\eta^3\text{-}C_4H_7)(\eta^4\text{-}C_4H_6)]^+$ active catalyst complex along the most feasible pathway (commencing from *anti*-PP and *syn*-PP isomers of **2c**, respectively; cf. Figure 3) together with Gibbs free energies (kcal mol^{-1}) relative to the most stable $[Ti^{III}(\eta^5\text{-}C_5H_5)(syn\text{-}\eta^3\text{-}C_4H_7)(\eta^4\text{-}cis\text{-}C_4H_6)]^+$ isomer of **2**.

feasible pathways for monomer insertion into the *anti*-butenyl− and *syn*-butenyl−Ti^{III} bonds of the respective routes are displayed in Figures 4 and 5. On the basis of the insights achieved for the critical elementary steps, the mechanistic implications for the cis−trans regulation as well as for the tacticity control of the 1,4-polymerization process will be elucidated.

I. Exploration of Crucial Elementary Steps. A. Butadiene π-Complex. The most stable form of the butadiene π-complex that was located is characterized (first) by the butenyl group in the η^3 mode and (second) by a bidentate coordination of the monomer. Thus, the $[Ti^{III}(\eta^5\text{-}C_5H_5)(\eta^3\text{-}C_4H_7)(\eta^4\text{-}C_4H_6)]^+$ species is the thermodynamically favorable form of the active catalyst complex (cf. Figures 4 and 5). Several other conceivable forms, with a η^1-σ-butenyl and/or η^2-butadiene coordination for example, which may be stabilized by coordination of the polybutadienyl chain, are found to be either thermodynamically less stable or to relax into the preferred η^3-π-butenyl/η^4-butadiene form. The butadiene is coordinated in an almost symmetrical fashion, with a similar Ti−C distance of all four carbons in case of the η^4-cis coordination, while for *trans*-butadiene the nonterminal carbons are distinctly closer to titanium than the terminal carbons. On the other hand, the butenyl−Ti^{III} coordination is characterized as occurring in a distorted η^3 mode, where the terminal reactive C^1 has a smaller distance to titanium in comparison with the substituted C^3. This unsymmetrical coordination has its primary origin in the influence of the polybutadienyl chain (mimicked by a methyl group in our catalyst model), which we consider to be predominantly steric in its nature, due to the interaction of the growing chain with the axial Cp ligand and/or the monomer moiety. This is revealed from the study of the $[Ti^{III}(\eta^5\text{-}C_5H_5)(\eta^3\text{-}C_3H_5)(\eta^4\text{-}C_4H_6)]^+$ catalyst model, where both the allyl group as well as butadiene (s-cis and s-trans configuration) is coordinated in a symmetrical fashion (cf. Figure S1 in the Supporting Information).

The stability of the butadiene π-complex is found to be essentially determined by the extent of the steric interactions of the butenyl and butadiene moieties with each other as well as with the axial Cp ligand. These interactions are likely to be less pronounced for *syn*-η^3-butenyl isomers when compared with *anti*-η^3-butenyl ones. Accordingly, the syn isomers are predicted to be thermodynamically preferred by ∼4.5−6.0 kcal mol^{-1} (ΔG) relative to the anti congeners for both η^4-*cis*-butadiene and η^4-*trans*-butadiene forms (cf. Table 1). Concerning the mutual orientation of the butenyl group and of butadiene, the respective isomers are seen to fall into a close energy interval. The isomers with a prone orientation of the two fragments, i.e., *anti*-PP and *syn*-PP, are predicted to be slightly favored among the several isomers for *cis*-butadiene forms, while the *Si*/*Si* and *Re*/*Si* isomers are the most stable ones for *anti*- and *syn*-butenyl η^4-*trans*-butadiene forms, respectively.

Overall, the favorable isomers of the *syn*-butenyl form are close in energy for η^4-cis and η^4-trans species (ΔG = 0.6 kcal mol^{-1}), and the same holds true for the thermodynamically less stable *anti*-butenyl form. Accordingly, η^4-cis and η^4-trans species of the active catalyst are indicated to exist in a comparable concentration under polymerization conditions, with the *syn*-η^3-butenyl form being prevalent and the anti form expected to be populated to a lesser extent. Therefore,

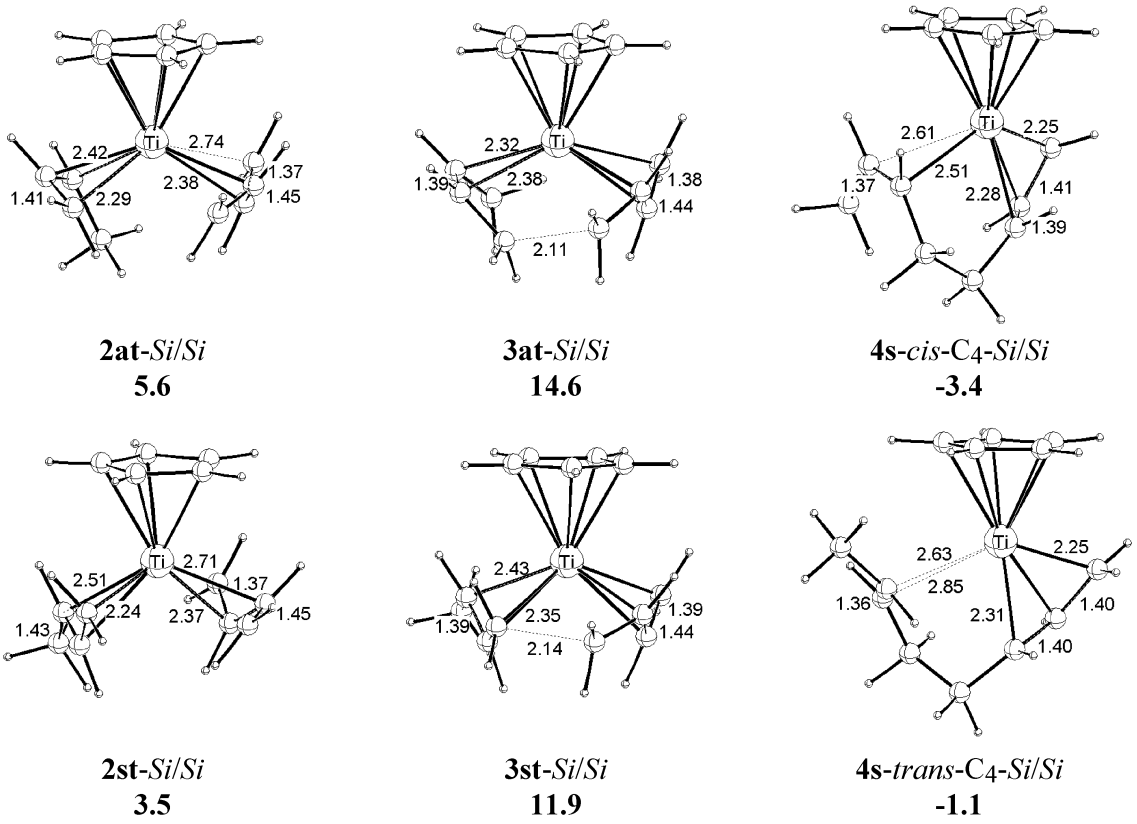

2at-*Si*/*Si* **3at**-*Si*/*Si* **4s**-*cis*-C$_4$-*Si*/*Si*
5.6 **14.6** **-3.4**

2st-*Si*/*Si* **3st**-*Si*/*Si* **4s**-*trans*-C$_4$-*Si*/*Si*
3.5 **11.9** **-1.1**

Figure 5. Selected geometric parameters (Å) of the optimized structures of key species for *trans*-butadiene insertion into the η^3-*anti*-butenyl−Ti^{III} bond (top) and into the η^3-*syn*-butenyl−Ti^{III} bond (bottom) of the [Ti^{III}(η^5-C_5H_5)(η^3-C_4H_7)(η^4-C_4H_6)]$^+$ active catalyst complex along the most feasible pathway (commencing from anti-*Si*/*Si* and syn-*Si*/*Si* isomers of **2t**, respectively; cf. Figure 3) together with Gibbs free energies (kcal mol^{-1}) relative to the most stable [Ti^{III}(η^5-C_5H_5)(*syn*-η^3-C_4H_7)(η^4-*cis*-C_4H_6)]$^+$ isomer of **2**.

on thermodynamic considerations the butadiene insertion is likely to have a similar probability of occurring from either the s-cis or the s-trans configuration.

B. Butadiene Insertion into the Butenyl−Ti^{III} Bond. Several conceivable pathways for this elementary process, which included explicitly η^1-σ-butenyl−Ti^{III} species as possible reactive intermediates, were tested. However, these species were found to be at high energy and were not indicated to be involved along any viable reaction path for this step. From the inspection of the key species that are involved along the most feasible pathway of the two competing paths for each of the reaction routes for insertion of *cis*-butadiene (cf. Figure 4) and of *trans*-butadiene (cf. Figure 5), it is obvious that in either case the insertion step commences from the η^4-butadiene π-complexes and then preferably takes place via the transition state **3** for butadiene insertion into the distorted η^3-butenyl reactive terminal group of the growing polybutadienyl chain. Thus, regardless of whether butadiene insertion occurs from the s-cis or s-trans configuration, it is clearly seen that the π-allyl-insertion mechanism[12,17] must be considered to be the operative of the two proposed mechanistic alternatives for the monomer insertion step for the actual allyltitanium(III) catalyst. Further support comes from the localized key species for the [Ti^{III}(C_5H_5)(C_3H_5)(C_4H_6)]$^+$ catalyst model (cf. Figure S1 in the Supporting Information), which unequivocally display the preferred η^3-π-mode of the allyl group in the transition state.

The most feasible pathway for butadiene insertion into the η^3-butenyl−Ti^{III} bond proceeds via a transition-state structure that is characterized by a quasi-planar four-membered cis arrangement of the butadiene's double bond that is inserted, the terminal reactive C^1 of the butenyl group, and the titanium atom. Accordingly, isomers with the *cis*-butadiene in prone orientation and the *trans*-butadiene *Si*-coordinated are involved along the most feasible pathway for the insertion of butadiene from the s-cis and s-trans configurations, respectively. This is due to the fact that for these cases the energetically favorable transition state can best be realized. In contrast, the pathways with supine *cis*-butadiene and *Re*-coordinated *trans*-butadiene isomers are connected with significantly higher activation barriers, since here an energetically unfavorable nonplanar four-membered transition-state structure is encountered. As a consequence, the proclivities of supine and prone η^4-*cis*-butadiene isomers to undergo monomer insertion (without mutual rearrangement of the butenyl and butadiene moieties) are significantly different, as indicated by the large gap between the respective barriers ($\Delta\Delta G^{\ddagger}$ > 10.0 kcal mol^{-1}, cf. Table 1), with the prone forms seen to be distinctly more reactive.

For insertion to occur via the preferred pathway, the required activation barrier is ∼6−7 kcal mol^{-1} ($\Delta\Delta G^{\ddagger}$, cf. Table 1) lower for the *cis*-butadiene route ($k_{c/t}$(cis)), as compared with that for the *trans*-butadiene insertion route ($k_{c/t}$(trans)). The corresponding transition states, both occurring at a distance of ∼2.1−2.2 Å of the emerging C−C σ-bond, display a different characteristic. The new terminal *anti*-butenyl group is essentially preformed in the transition-state structure for *cis*-

butadiene insertion, which thus appears product-like, while on the other hand the corresponding transition-state structure for the *trans*-butadiene route is characterized as being educt-like. Thus, the barrier accompanied by insertion of butadiene from the s-cis and s-trans configurations is reflected in the different degree of the monomer's conversion achieved in the transition state. Furthermore, insertion of both *cis*- and *trans*-butadiene is driven by a similar thermodynamic force that occurs in a slightly exergonic process. As a consequence, it must be concluded that, among the two routes, the insertion of *cis*-butadiene is favorable due to kinetic considerations, since it is connected with a distinctly lower activation barrier relative to the *trans*-butadiene insertion, which should be almost completely disabled. The similar concentration of the active catalyst species, together with the comparable reaction energies for the two routes, indicates that thermodynamic considerations are less important for determining which of the two routes is preferred.

Similar activation barriers have to be overcome along the preferred *cis*-butadiene insertion into the isomeric forms of the η^3-butenyl−Ti^{III} bond. The thermodynamically favorable syn form is likely to be only slightly more reactive relative to the anti form, since the total insertion barriers differ by no more than 1.4 kcal mol^{-1} ($\Delta\Delta G^{\ddagger}$; cf. Table 1) with the syn form being favored. Nearly identical total barriers of 6.0 kcal mol^{-1} ($\Delta G^{\ddagger}$) are connected with the preferred prone *cis*-butadiene pathways that involve supine and prone *syn*-butenyl isomers. On the other hand, the total activation barriers for the corresponding *anti*-butenyl isomers differ significantly ($\Delta\Delta G^{\ddagger} = 7.4$ and 12.1 kcal mol^{-1} for *anti*-PP/SP, respectively), which is due to an unfavorable steric interaction of the supine *anti*-butenyl group with the axial Cp ligand.

Overall, the chain propagation preferably takes place by *cis*-butadiene insertion into the η^3-butenyl−Ti^{III} bond via a quasi-planar four-membered transition state with butadiene in a prone orientation. A moderate, total activation barrier of 6.0−7.4 kcal mol^{-1} ($\Delta G^{\ddagger}$, relative to **2sc**-PP) has to be overcome in this process, which is exergonic by ∼-6.0 kcal mol^{-1}. The *anti*- and *syn*-butenyl forms should exhibit comparable reactivities, with the latter being slightly favorable; thus $k_t(\text{cis}) \gtrsim k_c(\text{cis})$ (cf. Scheme 1). The alternative insertion of *trans*-butadiene, however, is disfavored significantly, due to an insertion barrier that is ∼6−7 kcal mol^{-1} ($\Delta\Delta G^{\ddagger}$) higher; thus, $k_{c/t}(\text{cis}) \gg k_{c/t}(\text{trans})$ (cf. Scheme 1). Accordingly, the route for *trans*-butadiene insertion should be entirely disabled kinetically and is therefore not likely to have any significance in the catalytic reaction course of the 1,4-polymerization process.

C. Allylic Isomerization. As already mentioned in the general outline of the catalytic reaction cycle, the interconversion of the two isomeric anti and syn configurations of the terminal reactive η^3-allylic group of the growing polybutadienyl chain represents a crucial elementary process in the catalytic reaction course. Since *cis*-butadiene insertion is the preferred route for chain propagation, allylic isomerization is required for making the k_t(cis) path for generation of 1,4-trans polymer units accessible (cf. Scheme 1). The isomerization of the anti and syn forms of the η^3-butenyl−transition-metal bond is most likely to take place by means of a η^3-$\pi \rightarrow \eta^1(C^3)$-$\sigma$ conversion of the butenyl group, followed by an internal rotation of the vinyl group around the formal C^2-C^3 single bond (cf. Figure 6). There is both experimental[28] as well as theoretical[29] evidence for this preferred path of allylic isomerization.

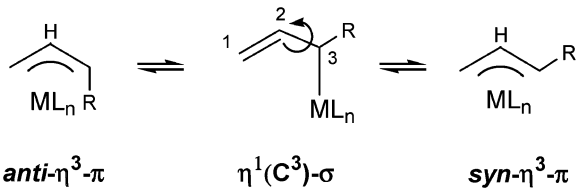

Figure 6. Interconversion of the anti and syn configurations of the η^3-butenyl−transition-metal bond via a $\eta^1(C^3)$-σ intermediate (R denotes the growing polybutadienyl chain).

Both anti and syn forms exist in equilibrium for the several species that are involved in the catalytic reaction course. The butadiene π-complex **2** and the insertion product **4a** are the likely candidates for allylic isomerization to occur. Commencing from these species, several pathways for this process were probed. The most feasible pathway was found to involve a rotational transition state that is stabilized by η^4-*cis*-butadiene coordination. The alternative coordination of the polybutadienyl chain's double bond from the ultimate and/or the penultimate inserted monomer, however, was seen to act less to stabilize the transition state. Therefore, it is most probable that isomerization takes place in the butadiene π-complex. It commences from the *anti*-η^3-butenyl−Ti^{III} species **2ac** (which is generated from the kinetic product of *cis*-butadiene insertion via k_c(cis) and k_t(cis) and subsequent monomer uptake) followed by rearrangement into the anti-$\eta^1(C^3)$ species and consecutive rotational isomerization through the $\eta^1(C^3)$ transition state **5c** to afford the syn-$\eta^1(C^3)$ species, which immediately rearranges into the thermodynamically most stable syn-η^3 species **2sc**. The careful exploration of the reaction path points out that, in contrast to rotational isomerization, the $\eta^3 \rightarrow \eta^1(C^3)$ rearrangement of the butenyl group (cf. Figure 6) does not involve a significant barrier and is driven entirely by the difference in the thermodynamic stabilities between the two species. We have not been able to locate the corresponding transition state.

The favorable isomer of **5c**, which constitutes the rotation of the vinyl group around the formal C^2-C^3 single bond in the $\eta^1(C^3)$ intermediate, is displayed in Figure 7 together with the corresponding species **2ac** and **2sc**. The possible additional, but weak, coordination of the growing polymer chain to the titanium atom in **5c** is found, however, to be unable to compensate for the loss of entropy that is associated with this process. Accordingly, the bidentate monomer complexation is the entire stabilizing factor of the transition state for allylic isomerization, while the polybutadienyl chain is not found to contribute in the facilitation of this elementary step. An activation barrier of 17.0 kcal mol^{-1} ($\Delta G^{\ddagger}$) has

(28) (a) Faller, J. W.; Thomsen, M. E.; Mattina, M. J. *J. Am. Chem. Soc.* **1971**, *93*, 2642. (b) Lukas, J.; van Leeuwen, P. W. N. M.; Volger, H. C.; Kouwenhoven, A. P. *J. Organomet. Chem.* **1973**, *47*, 152. (c) Vrieze, K. In *Dynamic Nuclear Magnetic Resonance Spectroscopy*; Jackman, L. M., Cotton, F. A., Eds.; Academic Press: New York, 1975.

(29) Tobisch, S.; Taube; R. *Organometallics* **1999**, *18*, 3045.

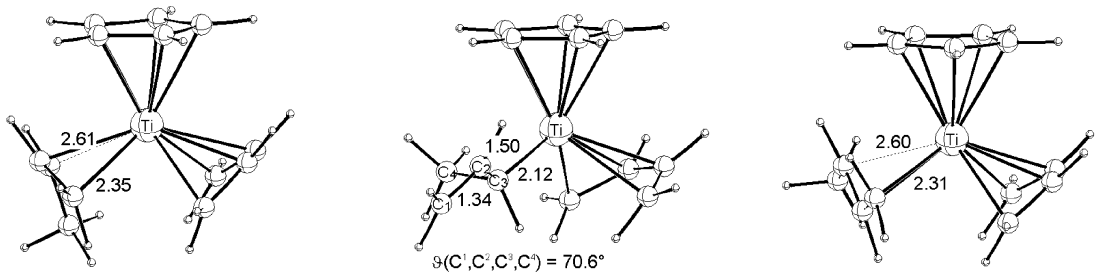

Figure 7. Selected geometric parameters (Å) of the optimized structures of key species for allylic anti−syn isomerization commencing from the *anti*-η^3 form **2ac** of the butadiene π-complex and occurring via the rotational $\eta^1(C^3)$ transition state **5c** together with Gibbs free energies (kcal mol^{-1}) relative to the most stable $[Ti^{III}(\eta^5\text{-}C_5H_5)(syn\text{-}\eta^3\text{-}C_4H_7)(\eta^4\text{-}cis\text{-}C_4H_6)]^+$ isomer of **2**.

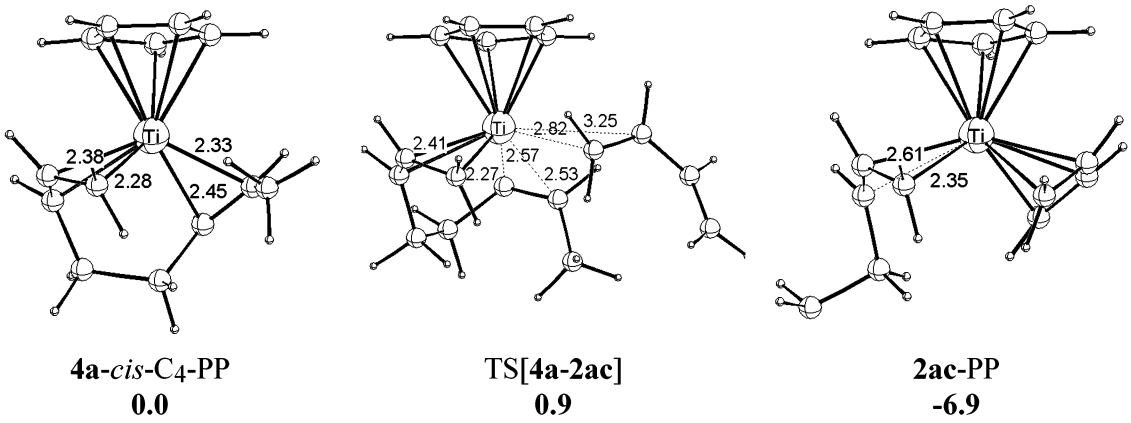

Figure 8. Selected geometric parameters (Å) of the optimized structures of key species for *cis*-butadiene uptake occurring in the kinetic *cis*-butadiene insertion product **4a** together with enthalpies (kcal mol^{-1}) relative to the separated (**4a**-*cis*-C_4-PP + *cis*-butadiene) moieties.

to be overcome for anti-syn isomerization relative to the most stable anti isomer **2ac**.

D. Monomer Uptake in the Insertion Product. The generation of the butadiene π-complex **2** as the starting point of a new chain propagation cycle, which proceeds via monomer uptake in the insertion product **4a**, represents a further important step during the catalytic reaction course. It has been argued in the context of the σ-allyl-insertion mechanism[2e,13] that the monomer uptake should be accompanied by the rearrangement of the reactive terminal polydienyl group from the η^3-allylic mode, as achieved in the insertion product, into the $\eta^1(C^1)$-allylic coordination mode in the monomer π-complex. A previous theoretical study[9e] on the same catalyst seems to support this mechanistic aspect. Moreover, the monomer uptake process was predicted to require a potential energy barrier of ~15 kcal mol^{-1} (ΔE) and was thus suggested as being the rate-determining step.[9e,30]

We have probed several pathways for the approach of a new *cis*-butadiene onto the Ti^{III} center of the *anti*-η^3-butenyl insertion product **4a** occurring along different directions. New butadiene is found to preferably coordinate in the equatorial coordination plane cis to the reactive terminal η^3-anti group of the polybutadienyl chain via a pathway that involves the monomer approach within this plane. In the first stage of the uptake process, the *cis*-butadiene coordinates weakly in a monodentate fashion and later easily rearranges into the preferred bidentate coordination mode. The transition state TS[**4a**-**2ac**] for *cis*-butadiene uptake occurs at a large distance between the approaching monomer and Ti^{III} (cf. Figure 8) in a very shallow region of the potential energy surface. Accordingly, several conformations of the transition state that lie energetically very close to each other ($\Delta E \approx 0.1-0.2$ kcal mol^{-1}) were located, which differ in the orientation as well as the enantioface of the incoming prochiral monomer. As can be clearly seen from Figure 8, the transition state for this process constitutes the uptake of a new *cis*-butadiene in the η^3-anti insertion product **4a** which is accompanied by a concerted displacement of the coordinated double bond of the polybutadienyl chain, arising from the monomer unit that is ultimately inserted. The minimum-energy pathway for the monomer uptake has been carefully explored going downhill toward both sides, commencing from the located transition state. There are no indications that the η^3-π coordination mode of the polybutadienyl terminal group achieved in the insertion product **4a** undergoes any significant rearrangement during the most feasible pathway for mono-

(30) To elucidate the discrepancy between our approach and previous[9e] theoretical studies, we have probed the different computational methodologies employed; viz. DFT(BP86) and ROHF, respectively, with regard to their ability in describing structural and energetic aspects of the allyl-titanium and butadiene-titanium coordination (cf. Supporting Information). This indicates that the ROHF method does not seem to be well suited in this regard, as it tends to predict the butadiene−titanium interaction to be too weak and to artificially favor the η^1-σ mode of the allyl−titanium coordination. Therefore, the mechanistic conclusions drawn in the previous study[9e] may have to be considered with some caution.

Scheme 2. Condensed Gibbs Free Energy Profile (kcal mol^{-1}) of the Proposed Catalytic Cycle of the 1,4-Polymerization of 1,3-Butadiene Assisted by the Cationic [Ti^{III}(η^5-C_5H_5)(η^3-RC_3H_4)(η^4-*cis*-C_4H_6)]$^+$ Active Catalyst Complex

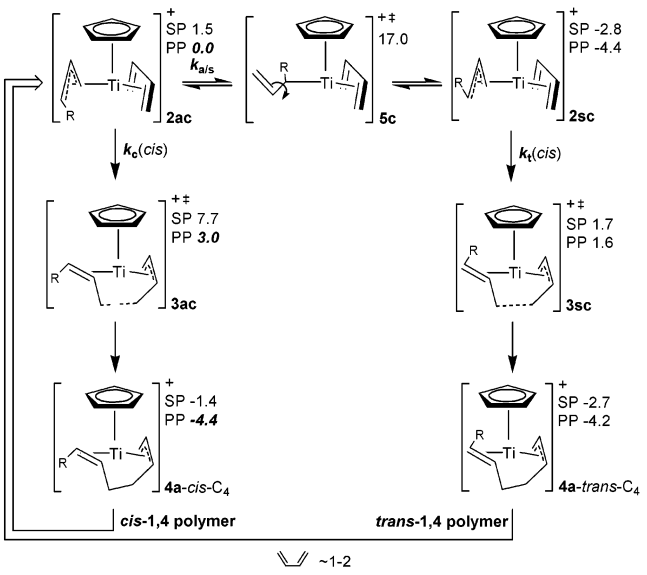

mer uptake. Commencing from the insertion product, the η^3-π mode is essentially preserved during the uptake process, giving rise to the *anti*-η^3-butenyl butadiene π-complex **2ac**.

The η^3-butenyl butadiene π-complex **2** is shown (first) to be thermodynamically favorable and (second) to represent the active form in the subsequent monomer insertion step. On the other hand, $\eta^1(C^1)$-σ forms, although repeatedly suggested as reactive intermediates,[3,9a−e,18] are not involved along viable pathways for the elementary processes of either monomer insertion or monomer uptake.

A very low enthalpic activation barrier of ∼0.9−1.1 kcal mol^{-1} ($\Delta H^{\ddagger}$)[31] relative to the separated fragments (**4a** + *cis*-butadiene) accompanies the approach and subsequent coordination of *cis*-butadiene to the insertion product **4a**. Furthermore, no significant entropy contribution is expected for the type of transition state associated with this process, one that constitutes the concerted attachment and detachment of double bonds to the Ti^{III} center without involving a larger rearrangement of the remaining ligand sphere. Therefore, the monomer uptake is indicated to be a facile process with a low activation barrier that occurs under preservation of the η^3-π coordination mode of the terminal polydienyl chain.

II. The Entire Catalytic Reaction Cycle. A. Free-Energy Profile. Now, the free-energy profile of the entire catalytic reaction course for the 1,4-polymerization of 1,3-butadiene assisted by the cationic allyltitanium(III) [Ti^{III}(η^5-C_5H_5)(η^3-RC_3H_4)(η^4-C_4H_6)]$^+$ catalyst is presented (cf. Scheme 2). This is based on the careful theoretical exploration of important elementary processes for the tentative polymerization cycle reported in previous sections. It consists of the most feasible pathways for each of these steps: namely, the *cis*-butadiene insertion into the η^3-butenyl−Ti^{III} bond occurring via competitive paths for formation of cis-1,4 (k_c(cis)) and trans-1,4 (k_t(cis)) polymer units, the anti−syn isomerization of the terminal polydienyl group via the $\eta^1(C^3)$-butenyl transition state **5c**, and the facile *cis*-butadiene uptake in the η^3-anti insertion product **4a**, affording the isomer **2ac** of the catalytically active butadiene π-complex to commence with a new chain propagation cycle. The intrinsic energy required to extend the polybutadienyl chain by an additional C_4 unit in consecutive propagation cycles is excluded from the energetic profile.[32] The allylic anti−syn isomerization is connected with the overall highest activation barrier of all important elementary steps, and the insertion product complex **4a** is predicted to act as the resting state under catalytic reaction conditions, since it represents the thermodynamically most stable complex in the catalytic reaction course.

B. Mechanism of Cis−Trans Regulation in the 1,4-Polymerization Process. The two isomeric η^3-anti and η^3-syn forms of the butenyl−Ti^{III} coordination are indicated to have a similar total reactivity when undergoing insertion of *cis*-butadiene, as seen from the small difference between the corresponding favorable transition-state structures ($\Delta\Delta G^{\ddagger} = 1.4$ kcal mol^{-1} in favor of the thermodynamically preferred η^3-syn form; cf. Table 1). Accordingly, the competing k_c(cis) and k_t-(cis) paths for generation of a new cis-1,4 and trans-1,4 C_4 unit should be crossed in comparable probabilities, giving rise to an equibinary polybutadiene consisting of similar amounts of cis-1,4- and trans-1,4-polymer units. For the trans-1,4 production path k_t(cis) to become accessible, however, a facile interconversion of the kinetically formed η^3-anti group (due to the *cis*-butadiene insertion) into the syn congener via **5c** is indispensable. The total activation barrier for isomerization is predicted to be 14.0 kcal mol^{-1} ($\Delta\Delta G^{\ddagger}$; cf. Scheme 2) higher than the activation energy for insertion along the most feasible pathway of the cis-1,4 path k_c(cis). Therefore, isomerization is likely to be much slower when compared with the *cis*-butadiene insertion into the η^3-butenyl−Ti^{III} bond. Consequently, the trans-1,4 production path k_t(cis) should be entirely precluded due to the slow allylic isomerization, affording nearly exclusively a *cis*-1,4-polybutadiene via the repeated *cis*-butadiene insertion into the *anti*-η^3-butenyl−Ti^{III} bond along k_c(cis). This is notwithstanding the fact that both η^3-anti and η^3-syn forms display a comparable reactivity. The monomer insertion via k_c(cis) is predicted to be the rate-determining elementary process in the catalytic reaction course, with the regeneration of the catalytically active species **2ac**, occurring through *cis*-butadiene uptake in **4a**, being a facile step. Furthermore, after a short initialization period, only anti forms should be detectable under polymerization conditions by NMR. The insertion product **4a**, which is characterized by a weak coordination of the first double bond of the polybutadienyl chain, is predicted to occur in highest concentration.

C. Rationalization of the Formation of Tactic *cis*-1,4-Polydienes. The catalyst under consideration

(31) For the transition state of the monomer uptake process with the weakly coordinating incoming monomer and the growing chain's double bond, entropy contributions cannot be reliably estimated by the theoretical method employed in this study.

(32) Compare the computational details; with the entropy contribution $T\Delta S$ amounts to 11.3 kcal mol^{-1}.

is known to promote the generation of a *cis*-1,4-polydiene for terminally monosubstituted butadienes, that is predominantly isotactic in its structure.[5a−c,6] The formation of a tactic polydiene can be envisioned to be determined by the chirality of the active center[2e] and thus by the enantiofaces of the two reactive butenyl and diene moieties that are involved in the C−C bond formation process. Multiple monomer insertions occurring via formation of the C−C bond between the same enantiofaces of the two fragments, for instance, produces a polydiene chain with chiral centers having identical configuration: i.e., an isotactic polydiene. In previous theoretical studies,[9a,f] the stabilizing effect of the coordinating polydienyl chain in the insertion product was thought to act as the regulating factor in the generation process of tactic polydienes. In contrast, we suggest a different plausible explanation of tacticity control in 1,4-polymerization on the basis of the presented exploration of individual elementary steps for the entire process.

As shown in section I, part B, the rate-determining step of the catalytic cycle, which is the *cis*-1,3-diene insertion into the *anti*-η^3-butenyl−Ti^{III} bond, preferably proceeds through the transition state **3ac**, which is characterized by a quasi-planar arrangement of the terminal carbon of the butenyl group, the Ti^{III} atom, and the inserting double bond of the 1,3-diene. This restricts the 1,3-diene to a prone orientation along the most feasible insertion pathway, while the η^3-butenyl group can be coordinated with either of its two enantiofaces. The axial Cp ligand, however, determines the *anti*-η^3-butenyl group's enantioface that is preferably involved in the C−C bond formation. In both the butadiene π-complex and also in the insertion transition state, the *anti*-η^3-butenyl group favorably adopts a prone orientation to minimize the destabilizing interaction with the axial Cp ligand. Therefore, the two reactive *anti*-η^3-butenyl and *cis*-1,3-diene fragments are most likely to coordinate with the same enantiofaces along the favorable pathway for the rate-determining insertion step (*anti*-PP stereoisomer; cf. Figure 4 (top)), which ensures the production of *cis*-1,4-polydiene in the case of 4-substituted butadienes that consists nearly exclusively of polymer units with identical chiral centers. Thus, the higher reactivity of the *cis*-1,3-diene in its prone orientation, together with the regulating influence of the axial Cp ligand, are suggested to be the decisive factors that control the possible tacticity in the 1,4-polymerization of 1,3-dienes assisted by the $[Ti^{III}Cp(polydienyl)(diene)]^+$ active catalyst.

Conclusion

We have presented a comprehensive theoretical investigation of the entire catalytic reaction course of the 1,4-polymerization of 1,3-butadiene with the cationic $[Ti^{III}(\eta^5\text{-}C_5H_5)(\eta^3\text{-}RC_3H_4)(\eta^4\text{-}C_4H_6)]^+$ complex as the active catalyst, employing a gradient-corrected DFT method. Crucial elementary processes have been carefully explored for a tentative catalytic cycle, namely monomer insertion, allylic anti−syn isomerization, and monomer uptake. The most feasible among the several possible pathways for each of these steps are predicted, with special emphasis directed at elucidating the role played by η^3-π-butenyl− and η^1-σ-butenyl−Ti^{III} species in the catalytic reaction course. This leads us to propose a theoretically verified catalytic cycle for 1,4-polymerization of 1,3-butadiene for the actual allyltitanium(III) catalyst, which provides a consistent rationalization of the experimental observation. The present theoretical study contributes (first) to a more detailed understanding of mechanistic aspects of the allyltitanium(III)-catalyzed 1,4-polymerization of 1,3-dienes, with the mechanism of stereoregulation in particular, and (second) to a deeper insight into the catalytic structure−reactivity relationships in the transition-metal-assisted 1,3-diene polymerization.

The following mechanistic aspects, which remained unresolved from both experiment and previous theoretical studies, are clarified.

(1) The chain propagation preferably takes place via butadiene insertion into the η^3-butenyl−Ti^{III} bond, while $\eta^1(C^1)$-σ-butenyl−Ti^{III} species, which were suggested as reactive intermediates, are not involved along the most feasible path for the monomer insertion step. Thus, the π-allyl-insertion mechanism is verified as being the operative of the two proposed mechanisms.

(2) Both the alternative *cis*- and *trans*-butadiene insertion routes are indicated to be likely as well, on thermodynamic considerations. However, the insertion of *cis*-butadiene is predicted to be distinctly favored on kinetic grounds over that for the insertion of *trans*-butadiene. An *anti*-η^3-butenyl group is generated as the reactive end of the growing polybutadienyl chain in the kinetic *cis*-butadiene insertion product, which is stabilized by the coordination of the first chain's double bond to the Ti^{III} center.

(3) A quasi-planar four-membered transition-state structure with *cis*-butadiene in prone orientation is encountered along the most feasible insertion pathway that is connected with a moderate free energy barrier of 3.0 kcal mol^{-1}. The two isomeric *syn*-η^3-butenyl− and *anti*-η^3-butenyl−Ti^{III} forms display comparable reactivities to undergo *cis*-butadiene insertion ($\Delta\Delta G^{\ddagger} = 1.4$ kcal mol^{-1}) with the thermodynamically favorable syn-η^3 form indicated to be only slightly more reactive.

(4) The allylic isomerization preferably proceeds by commencing from the butadiene π-complex via a $\eta^1(C^3)$-butenyl−Ti^{III} rotational transition state. This process is indicated to be much slower than the *cis*-butadiene insertion, due to a total barrier for anti−syn isomerization that is 14.0 kcal mol^{-1} ($\Delta\Delta G^{\ddagger}$) higher. Consequently, the *trans*-1,4 generating path k_t(cis) is entirely precluded, since the syn form is prevented from being generated in appreciable concentration.

(5) The regeneration of the butadiene π-complex as the catalytically active species for the next chain propagation cycle takes place via a facile *cis*-butadiene uptake ($\Delta G^{\ddagger} \approx 1-2$ kcal mol^{-1}) in the *anti*-η^3-butenyl−Ti^{III} insertion product, which occurs with preservation of the η^3-π-coordination of the reactive terminal group of the growing polybutadienyl chain.

(6) The entire formation of *anti*-η^3-butenyl forms as the result of the favorable *cis*-butadiene insertion route and the slow allylic anti−syn isomerization are the decisive factors for the nearly exclusive generation of a *cis*-1,4-polybutadiene, notwithstanding of the comparable reactivity of *anti*-η^3- and *syn*-η^3-butenyl forms. The *cis*-butadiene insertion into the *anti*-η^3-butenyl−Ti^{III} bond is predicted to be rate-controlling, with the *anti*-

η^3-butenyl insertion product likely to represent the catalyst's resting state.

(7) The formation of a stereoregular isotactic *cis*-1,4-polydiene, for 1,3-butadienes that are terminally monosubstituted, can be rationalized in terms of the higher reactivity of the *cis*-1,3-diene in its prone orientation together with the regulating influence of the axial Cp ligand.

Acknowledgment. I am grateful to Prof. Dr. Rudolf Taube for his ongoing interest in this research, which serves as a continuous source of stimulation. Excellent service by the computer centers URZ Halle and URZ Magdeburg is gratefully acknowledged. I thank the Deutsche Forschungsgemeinschaft (DFG) for financial support by an Habilitandenstipendium.

Supporting Information Available: Full descriptions of the geometry of all reported species and the calculated free-energy profile for the monomer insertion step of the 1,4-polymerization of 1,3-butadiene for the $[Ti^{III}(\eta^5\text{-}C_5H_5)(\eta^3\text{-}C_3H_5)(\eta^4\text{-}C_4H_6)]^+$ active catalyst complex together with the pictorial representation of the key species involved (Table S1, Figure S1) and a comparison of different computational methodologies with respect to their ability in reproducing structural and energetic aspects of the allyl−titanium and the butadiene−titanium coordination (Figures S2 and S3). This material is available free of charge via the Internet at http://pubs.acs.org.

OM030059P